第 51 卷 第 12 期/2024 年 6 月/中国激光 研究论文

中国激光

光束质量对铝合金激光焊接效率与良率的影响

张帅[1,2]，刘同争[1]，徐志宏[1]，代小光[1]，朱朝晖[1]，高明[2*]，郭少锋[1]

[1]湖南大科激光有限公司，湖南 湘阴 414615；

[2]华中科技大学武汉光电国家研究中心，湖北 武汉 430074

摘要 为了满足当前新能源动力电池高速生产线极限制造的需求，基于激光焊接过程中的能量分布特征，系统分析了铝合金激光焊接中光纤激光器的光束质量效应，研究了光束质量与焊接稳定性和焊接效率之间的定量关系。随着激光器光束质量因子(M^2)的减小，焊缝熔深为2.7 mm时焊接速度呈增大趋势，焊接熔深的工序能力指数(CPK)值也呈增大趋势；当M^2从11.60减小到1.25时，焊缝熔深为2.7 mm时激光器的焊接速度增加了5.5倍，焊接熔深CPK值提升了2.3倍。基于激光能量分布特征的分析结果，激光器光束质量效应的提升机制为：在保持相同熔深的条件下，M^2越小，能量密度极大值越大，且焊道边缘与中间区域之间的能量密度极值差越大，工件材料的能量吸收效率会越高，则激光器的焊接效率越高。提出将激光器能量密度极大值和能量密度极值差这两者的乘积作为激光器能量密度焊接效率影响因子，由理论计算可知，M^2为1.18时的激光器能量密度焊接效率影响因子比M^2为11.6时的增加了5.2倍，与实验结果基本一致。

关键词 激光技术；激光焊接；光束质量；能量分布；铝合金

中图分类号 TG456.7 **文献标志码** A **DOI**：10.3788/CJL230909

1 引 言

随着世界能源危机和环境污染问题的加剧，全球新能源的开发与利用正加速发展。锂电池作为新一代绿色新能源产品在碳中和背景下即将迈入TW·h(亿千瓦时，即1000 GW·h)时代[1-4]。在新能源汽车领域，2022年全球电动汽车动力电池的装机量约为518 GW·h，同比增长71.8%，预测2025年全球动力电池装机量将达1485 GW·h，产能为1782 GW·h。同时，在新基建储能电池领域，锂电池装机总规模为动力电池市场体量的40倍。动力电池对新能源汽车的续航里程、整车寿命、安全性、成本等关键指标均有非常重要的影响，提升动力电池性能和生产效率是提升新能源汽车市场竞争力的关键。当前，主流新能源电池厂家的产能达到了200 PPM(Pieces Per Minute)，未来圆柱电池的产能计划将提升至300 PPM，那么如此高速的生产线极限制造对焊接工艺也提出了极大的挑战。因此，高效率和高可靠性的电池焊接技术和工艺成为汽车制造业发展亟待解决的问题。激光焊接由于激光光斑小、能量密度高，焊接效率高，焊缝深宽比大，且输入量小，工件变形小，焊接能量可精确控制，自动化程度高，安全性高等，在新能源电池焊接乃至整车制造等领域中有着广泛的应用[5-6]。

新能源电池焊接材料主要是1系和3系铝合金，由于铝合金对激光的反射率较高，在焊接过程中，易出现熔池飞溅、爆点、虚焊、气孔、烧穿等现象[7-8]。Zhou等[9]采用光纤激光摆动模式焊接了2 mm厚的铝合金2060板材，发现“8”形摆动模式细化了晶粒，焊接接头的抗拉强度提升到338 MPa，比无摆动焊接提高了68%。耿立博[10]开展了高功率密度激光焊接动力电池防爆阀的研究，发现冲压加工后残留的冲压油、清洁液等液体极易气化并上浮到熔池表面，爆裂的同时产生大量飞溅并在焊缝表面留下凹坑，造成了焊接过程的不稳定性。王天鸽等[11]开展了真空环境下的5083铝合金厚板激光焊接研究，发现降低环境压力可明显改善焊缝表面形貌，减少焊接缺陷，焊缝熔深提高2倍，气孔率降低到0.057%。邹吉鹏等[12]开展了厚板铝合金5A06的激光摆动窄间隙填丝焊接研究，发现当激光束采用圆形摆动模式且扫描频率为300 Hz时，焊接过程的稳定性得到提高，焊缝侧壁未熔合、裂纹等焊接缺陷显著减少，气孔率降低至1%。Huang等[13]开展了铝合金5083的激光焊接研究，通过数值模拟分析，发现焊前预热可以提高匙孔稳定性并促进气泡溢出，进而降低了气孔率。当前的研究主要是通过激光焊接工艺参数的优化和光束的整形来提高铝合金的焊接质量，工艺参数优化包含激光功率

收稿日期：2023-06-12；**修回日期**：2023-08-07；**录用日期**：2023-09-05；**网络首发日期**：2023-09-15

基金项目：国家自然科学基金(52205465)

通信作者：*mgao@mail.hust.edu.cn

和焊接速度匹配、脉冲调制、激光焦点光斑优化等[14-19]，但随着人们对动力电池焊接效率的要求越来越高，同时保证焊接质量和焊接速度的工艺窗口将会越来越窄，甚至很难找到合适的工艺参数窗口，亟须另辟蹊径。考虑到激光器作为一种新型的焊接光源，与电弧焊机产生的弧光光源相比还是有一定的特性差异，而目前的研究主要关注的是激光器的功率大小，关于激光光源本身的特性对焊接质量和效率的影响，尤其是激光器光束质量效应的研究还未见相关报道。

因此，本文首先研究了激光焊接速度对铝合金焊缝熔深和熔宽的影响，其次研究了激光器光束质量对铝合金焊接稳定性和焊接效率的影响，进而通过仿真分析了焊接过程中的能量分布图，建立了激光器光束质量与焊接稳定性和焊接效率的定量关系，并系统探讨了光束质量对铝合金激光焊接效率的提升机制，为新能源动力电池的高速高效激光焊接提供了参考。

2 实验条件

2.1 实验设备

实验所用的激光器为工业级 3 kW 连续光纤激光器，激光波长为 1080 nm，离焦量为 0 mm。采用的焊接振镜的场镜焦距为 420 mm，准直焦距为 150 mm，激光器的其他参数如表 1 所示，其中 M^2 为光束质量因子。本实验采用圆形摆动路径进行激光焊接，摆动幅度为 0.6 mm、摆动间距为 0.25 mm，光束圆形摆动形成的焊接路径的示意图如图 1 所示。

表 1 激光器参数

Table 1 Laser parameters

No.	Core diameter of fiber /μm	Welding power /kW	Beam quality factor M^2	Output mode	Beam spot size /mm
1	100	2.8	11.60	Multimode	0.364
2	100	2.8	6.76	Multimode	0.215
3	50	2.8	6.60	Multimode	0.109
4	50	2.8	2.45	Multimode	0.092
5	20	2.8	1.25	Single mode	0.046
6	20	2.8	1.18	Single mode	0.044

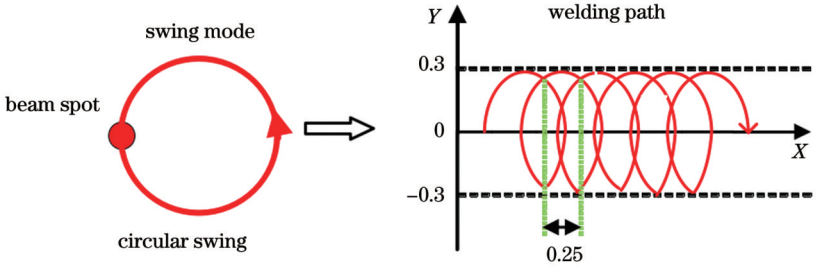

图 1 光束圆形摆动形成的焊接路径的示意图

Fig. 1 Schematic of welding path formed by circular swing of beam

2.2 实验材料及方法

实验采用叠焊的方式，上层材料为 1.5 mm 厚的 3003 铝合金板材，下层材料为 3 mm 厚的 3003 铝合金板材，板材尺寸为 50 mm×30 mm，接头形式为搭接，材料的化学成分如表 2 所示。焊前在试件表面上用钢刷和砂纸去除氧化皮并进行抛光，再用乙醇和丙酮擦拭干净。采用氩气作为上表面侧吹气和背部保护气，侧吹气体和背部保护气体的流量均为 25 L/min。测试激光器焊接铝合金良率的工序能力指数(CPK)值采用的焊接工艺参数如表 3 所示。CPK 值的计算公式为

$$C_{PK}=C_P(1-k)=\frac{T-2\varepsilon}{6S},\tag{1}$$

式中：C_{PK} 为 CPK 值；$C_p=(T_U-T_L)/(6S)$，其中 S 为样本标注差，T_U 为上限值，T_L 为下限值；k 为相对偏移量，$k=2\varepsilon/T$，其中 T 为工艺参数规范范围，$T=T_U-T_L$，ε 为绝对偏移量，$\varepsilon=|M-\mu|$，M 为公差带中心，$M=(T_U-T_L)/2$，μ 为目标值。

表 2 3003 铝合金的主要化学成分

Table 2 Main chemical compositions of 3003 aluminum alloy

Chemical composition	Mn	Si	Fe	Cu	Zn	Al
Mass fraction /%	1.00–1.50	0.60	0.70	0.05–0.20	0.10	Bal.

表 3 激光器焊接铝合金的CPK测试参数

Table 3 Parameters for testing CPK in laser welding of aluminum alloy

No.	Beam quality fator M^2	Sample number	Upper limit /mm	Lower limit /mm	Subgroup size	Welding speed /(mm/s)
1	11.60	32	3	2.5	5	40
2	6.76	32	3	2.5	5	60
3	6.60	32	3	2.5	5	84
4	2.45	32	3	2.5	5	175
5	1.25	32	3	2.5	5	262
6	1.18	32	3	2.5	5	228

3 实验结果与分析

3.1 光束质量对焊缝成形的影响

光束质量对焊缝表面形貌和焊缝横截面形貌的影响如图 2 所示。可以看出：当激光器的 M^2 为 1.18 时，焊缝表面形貌随焊接速度(v)的变化较小，也没有明显驼峰现象，但焊缝表面不平滑；当 M^2 增加到 1.25 时，焊缝表面开始出现驼峰，且随着焊接速度的增加，驼峰现象更加明显，焊缝表面质量较差；当 M^2 增加到 2.39 以上时，焊缝表面比较平滑，无驼峰现象出现；当 M^2 小于 6.74 时，焊接过程中无明显飞溅现象；当 M^2 增加到 6.74 时，开始出现明显的飞溅，且随着焊接速度的增加，飞溅有一定的改善。从焊缝的横截面可以看出：当激光器的 M^2 一定时，焊缝的截面形貌随焊接速度的变化较小；随着 M^2 的增加，焊缝的深宽比明显减小；当 M^2 为 1.25 时，焊缝的余高比较明显，且随着焊接速度的增加，余高部分的截面积增大；当 $1.25<M^2<6.74$ 时，焊缝的余高较小，也没有明显的凹陷；当 M^2 增加到 6.74 时，焊缝表面边缘开始出现部分凹陷。

光束质量对焊缝熔深和熔宽的影响如图 3 所示。激光器光束质量与光纤的芯径和数值孔径息息相关，光纤芯径越小，光束质量越易提高，获得的 M^2 越小。可以看出：当光纤芯径为 20 μm 时，M^2 对焊缝熔深的影响较小，而在相同的焊接速度下，M^2 为 1.18 时对应的焊缝熔宽均比 M^2 为 1.25 时的大；当光纤芯径为 20 μm 且焊接速度为 228 mm/s 时，与 M^2 为 1.25 的试样相比，M^2 为 1.18 的试样的焊缝熔宽和熔深两者之间的差值较大，焊缝熔宽增加了 26.6%，焊缝熔深减小了 8.7%；当光纤芯径为 50 μm 时，在相同的焊接速度下 M^2 为 2.39 的试样的焊缝熔深均比 M^2 为 6.6 的大，M^2 为 2.39 的试样的焊缝熔宽均比 M^2 为 1.25 的小，且随着焊接速度的增加，焊缝熔深和熔宽均呈减小的趋势；当光纤芯径为 50 μm 且焊接速度为 80 mm/s 时，M^2 为 2.39 的试样的焊缝熔深比 M^2 为 6.6 的增大了 22.7%，M^2 为 2.39 的试样的焊缝熔宽比 M^2 为 6.6 的减小了 2.5%；当光纤芯径为 100 μm 时，在相同的焊接速度下，M^2 为 6.74 的试样的焊缝熔深均比 M^2 为 11.6 的大，两者的熔宽差较小，且随着焊接速度的增加，焊缝熔深和熔宽也均呈减小的趋势；当光纤芯径为 100 μm 且焊接速度为 60 mm/s 时，M^2 为 6.74 的试样的焊缝熔深比 M^2 为 11.6 的增大了 9.9%，M^2 为 6.74 的试样的焊缝熔宽比 M^2 为 11.6 的减小了 12.1%。

3.2 光束质量对激光器焊接效率和CPK值的影响

为了统一分析激光器的焊接效率，我们选取焊缝熔深均为 2.7 mm 时对应试样的焊接速度，对比分析了不同光束质量下的激光器焊接效率，如图 4(a)所示。可以看出：随着激光器 M^2 的增加，焊缝熔深为 2.7 mm 时对应的焊接速度呈减小趋势，当 $1.25\leqslant M^2\leqslant 6.60$ 时，焊接速度随 M^2 的增加快速减小，当 $6.74\leqslant M^2\leqslant 11.60$ 时，焊接速度随 M^2 的增加缓慢减小；当 M^2 从 11.60 减小到 1.25 时，焊缝熔深为 2.7 mm 时对应的激光器的焊接速度增加了 5.5 倍。光束质量对激光器焊接良率CPK值的影响如图 4(b)所示。可以看出：随着激光器 M^2 的增加，激光器焊接熔深CPK值也呈减小趋势，当 $1.25\leqslant M^2\leqslant 6.60$ 时，CPK值随 M^2 的增加快速减小，当 $6.74\leqslant M^2\leqslant 11.60$ 时，CPK值随 M^2 的增加缓慢减小；当 M^2 从 11.60 减小到 1.25 时，激光器焊接熔深CPK值提升了 2.3 倍；随着激光器 M^2 的增加，激光器焊接熔宽CPK值也呈先增大后减小的趋势，当 $2.39\leqslant M^2\leqslant 6.74$ 时，激光器焊接熔宽CPK值随 M^2 的增加快速减小，当 $6.74<M^2\leqslant 11.60$ 时，激光器焊接熔宽CPK值随 M^2 的增加缓慢减小；当 M^2 从 11.60 减小到 2.39 时，激光器焊接熔宽CPK值增加了 3.1 倍。

3.3 激光器光束质量效应的提升机制

在激光焊接过程中，激光的能量分布不均匀导致焊接不稳定，甚至出现飞溅、咬边、凹陷等缺陷[20]。另外，激光能量密度是表征激光焊接能量分布的重要参量，也是影响焊缝形貌的主要因素[21]。本文基于华中科技大学高明团队开发的能量分布特征分析软件，得

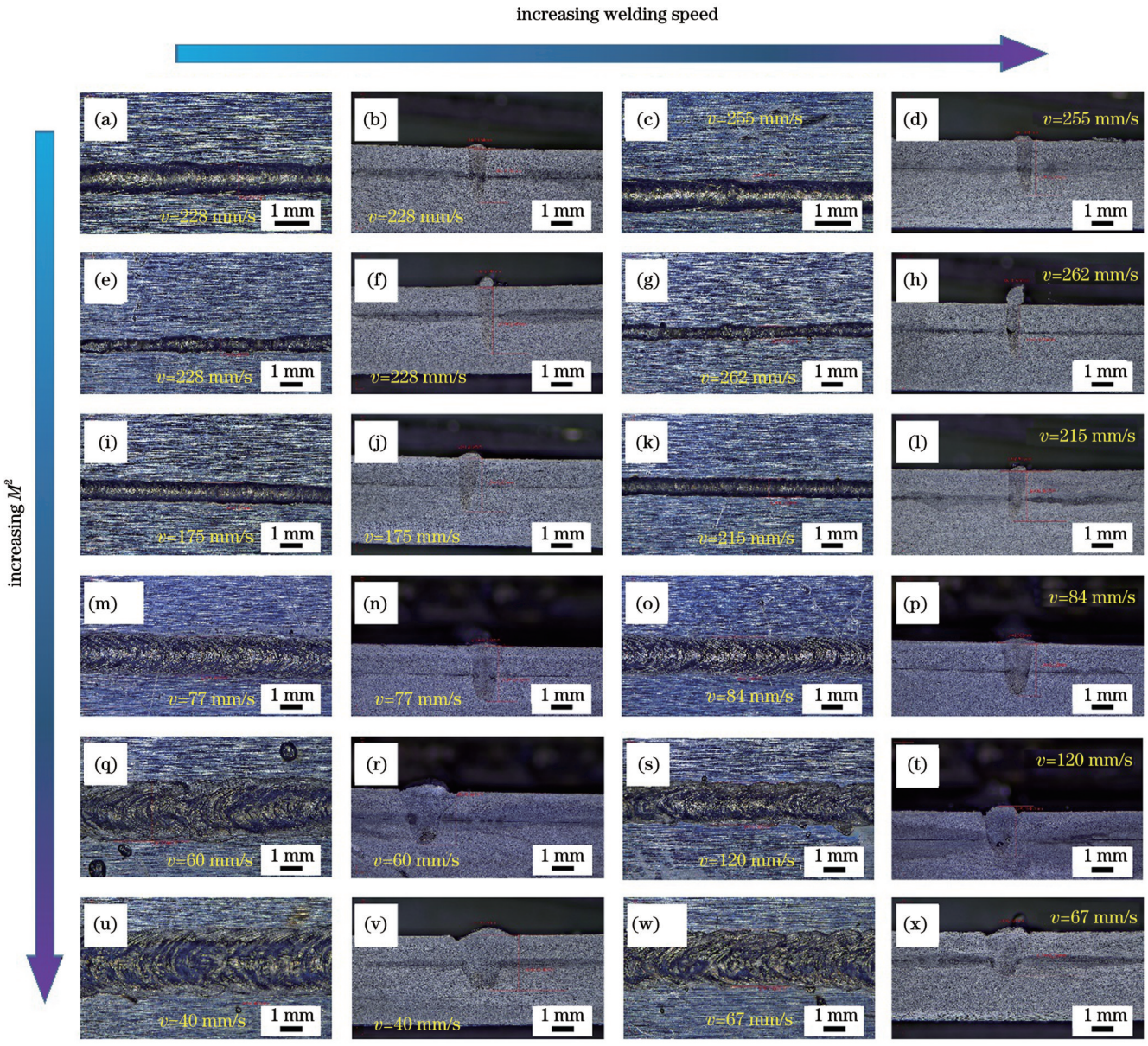

图 2 焊接速度和 M^2 对焊缝表面形貌、焊缝形貌的影响。表面形貌：(a) M^2=1.18，v=228 mm/s；(c) M^2=1.18，v=255 mm/s；(e) M^2=1.25，v=228 mm/s；(g) M^2=1.25，v=262 mm/s；(i) M^2=2.39，v=175 mm/s；(k) M^2=2.39，v=215 mm/s；(m) M^2=6.6，v=77 mm/s；(o) M^2=6.6，v=84 mm/s；(q) M^2=6.74，v=60 mm/s；(s) M^2=6.74，v=120 mm/s；(u) M^2=11.6，v=40 mm/s；(w) M^2=11.6，v=67 mm/s。熔深和熔宽：(b) M^2=1.18，v=228 mm/s；(d) M^2=1.18，v=255 mm/s；(f) M^2=1.25，v=228 mm/s；(h) M^2=1.25，v=262 mm/s；(j) M^2=2.39，v=175 mm/s；(l) M^2=2.39，v=215 mm/s；(n) M^2=6.6，v=77 mm/s；(p) M^2=6.6，v=84 mm/s；(r) M^2=6.74，v=60 mm/s；(t) M^2=6.74，v=120 mm/s；(v) M^2=11.6，v=40 mm/s；(x) M^2=11.6，v=67 mm/s

Fig. 2 Influence of welding speed and M^2 on weld surface morphology and weld morphology. Surface morphology: (a) M^2=1.18, v=228 mm/s; (c) M^2=1.18, v=255 mm/s; (e) M^2=1.25, v=228 mm/s; (g) M^2=1.25, v=262 mm/s; (i) M^2=2.39, v=175 mm/s; (k) M^2=2.39, v=215 mm/s; (m) M^2=6.6, v=77 mm/s; (o) M^2=6.6, v=84 mm/s; (q) M^2=6.74, v=60 mm/s; (s) M^2=6.74, v=120 mm/s; (u) M^2= 11.6, v=40 mm/s; (w) M^2=11.6, v=67 mm/s. Melting depth and width: (b) M^2=1.18, v=228 mm/s; (d) M^2=1.18, v=255 mm/s; (f) M^2=1.25, v=228 mm/s; (h) M^2=1.25, v=262 mm/s; (j) M^2=2.39, v=175 mm/s; (l) M^2=2.39, v=215 mm/s; (n) M^2=6.6, v=77 mm/s; (p) M^2=6.6, v=84 mm/s; (r) M^2=6.74, v=60 mm/s; (t) M^2=6.74, v=120 mm/s; (v) M^2=11.6, v=40 mm/s; (x) M^2=11.6, v=67 mm/s

到了图 5 所示的圆形摆动激光焊接能量分布的特征图。可以发现：在 XOY 面上，上下两边缘处的激光能量明显高于中间区域，中间区域有呈排状分布的明亮条纹，且激光器 M^2 越大，边缘的能量越集中，中间区域的明亮条纹越密集。在 XOZ 面上，当 $1.18\leqslant M^2\leqslant 1.25$ 时，能量密度极值点分布曲线不顺滑；当 $2.39\leqslant M^2\leqslant 11.60$ 时，能量密度极值点分布曲线明显顺滑。在 YOZ 面上，随着激光器 M^2 的增大，左右两侧的能量密

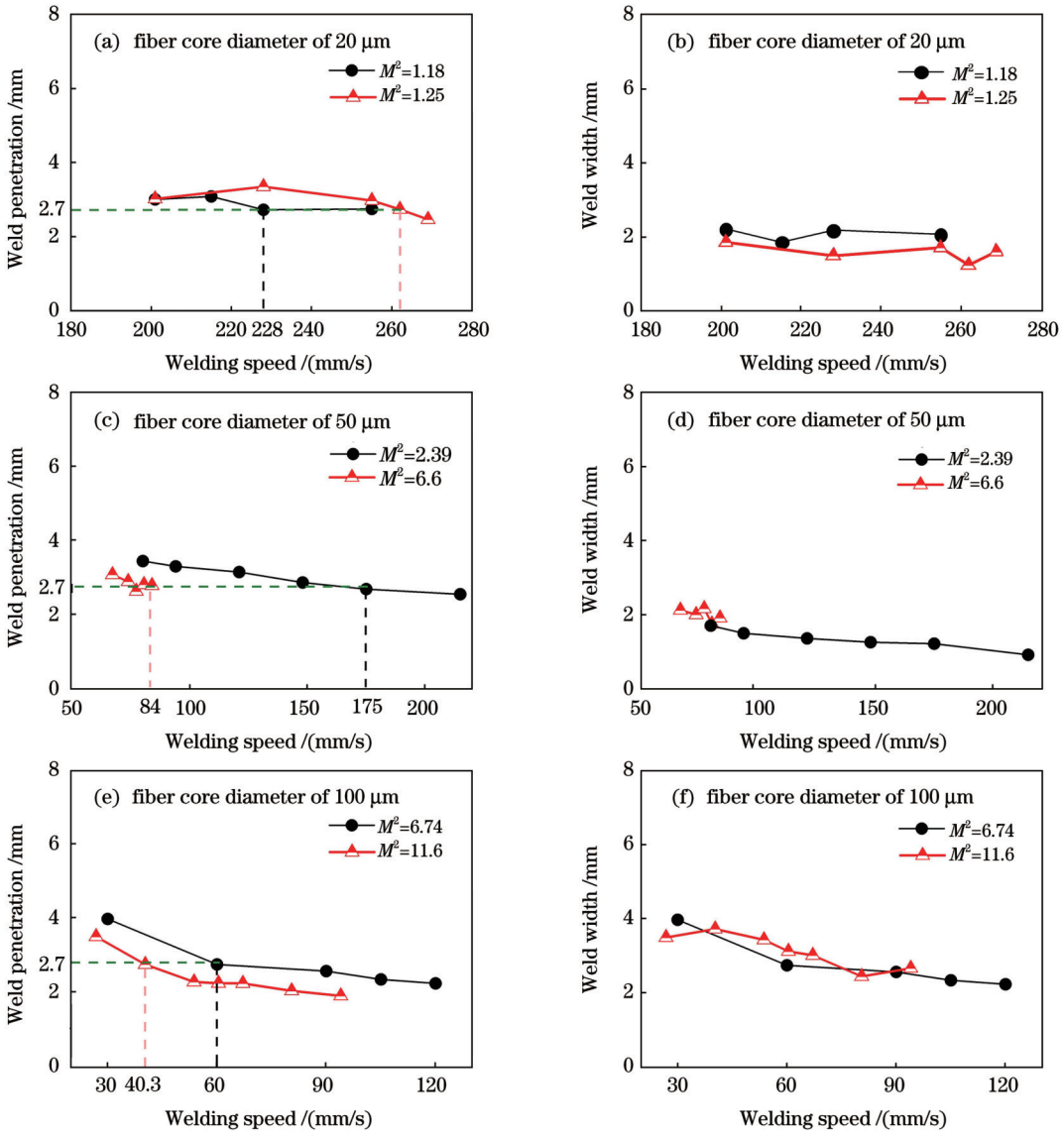

图 3　M^2对焊缝熔深、熔宽的影响

Fig. 3　Influence of M^2 on weld penetration and weld width

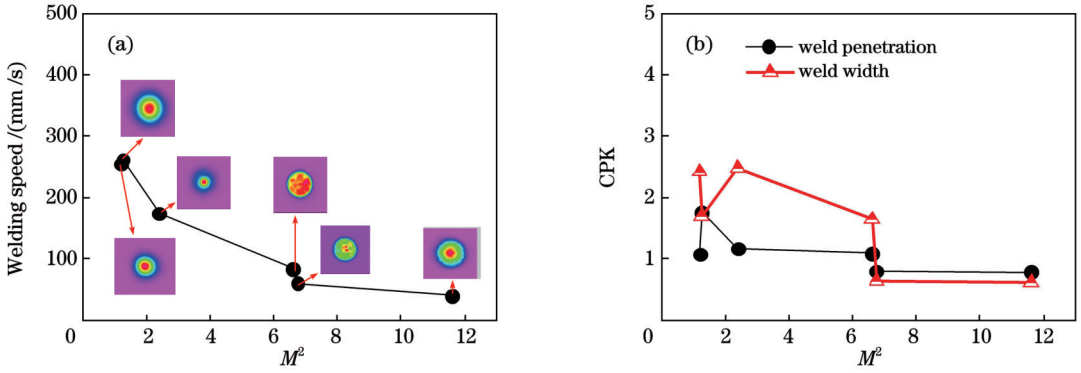

图 4　M^2对激光器焊接效率和CPK值的影响。(a)焊接速度;(b) CPK值

Fig. 4　Influence of M^2 on laser welding efficiency and CPK value. (a) Welding speed; (b) CPK value

度极大值基本呈减小的趋势,且两个极大值之间的区域的面积减小;M^2为1.18时的能量密度极大值比M^2为11.6时的增加了1.4倍。为了系统研究能量密度分布对激光焊接效率和良率的影响,本文计算了YOZ面左右两侧边缘的能量密度极大值与中间区域的能量密度极小值的差值,结果如图6所示。可以看出:随着激光器M^2的增大,能量密度极值差也基本呈减小的趋势,当$1.18\leqslant M^2\leqslant 6.60$时,能量密度极值差随$M^2$的增

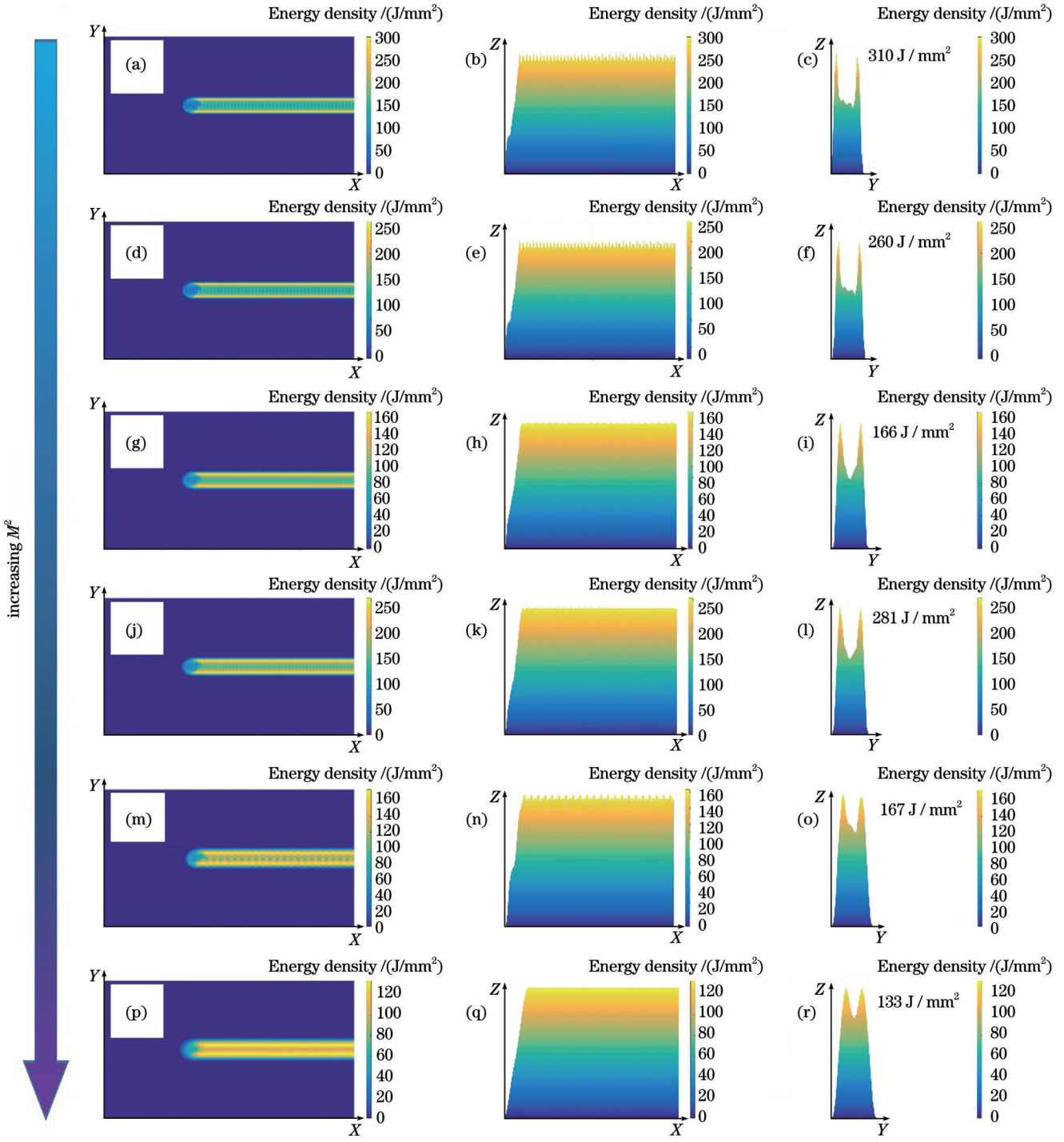

图 5 M^2对铝合金激光焊接能量分布特征的影响。XOY面:(a) M^2=1.18;(d) M^2=1.25;(g) M^2=2.39;(j) M^2=6.60;(m) M^2=6.74;(p) M^2=11.6。XOZ面:(b) M^2=1.18;(e) M^2=1.25;(h) M^2=2.39;(k) M^2=6.60;(n) M^2=6.74;(q) M^2=11.6。YOZ面:(c)M^2=1.18;(f) M^2=1.25;(i) M^2=2.39;(l) M^2=6.60;(o) M^2=6.74;(r) M^2=11.6

Fig. 5 Influence of M^2 on energy distribution characteristic in laser welding of aluminum. XOY plane: (a) M^2=1.18; (d) M^2=1.25; (g) M^2=2.39; (j) M^2=6.60; (m) M^2=6.74; (p) M^2=11.6. XOZ plane: (b) M^2=1.18; (e) M^2=1.25; (h) M^2=2.39; (k) M^2=6.60; (n) M^2=6.74; (q) M^2=11.6. YOZ plane: (c) M^2=1.18; (f) M^2=1.25; (i) M^2=2.39; (l) M^2=6.60; (o) M^2=6.74; (r) M^2=11.6

大快速减小,当6.74≤M^2≤11.60时,能量密度极值差随M^2的增大缓慢减小;M^2为1.18时的能量密度极值差比M^2为11.6时的增加了3.7倍。在激光焊接中,激光焊接的效率取决于激光与材料的相互作用程度。对于铝合金来说,由于铝合金对激光的反射率较高,故只有当激光的能量密度大于激光能量密度阈值时,铝合金工件表面的材料才能快速熔化,且随着工件温度的快速升高,工件的能量吸收率也快速增大。另外,随着激光能量密度的增加,熔池内的整体温度升高,这进一步减小了焊接方向的温度梯度,平衡了温度场,起到了稳定匙孔的作用,所以铝合金的焊接效率得到快速的提升[22]。在圆形摆动激光焊接中,光束的圆形摆动造

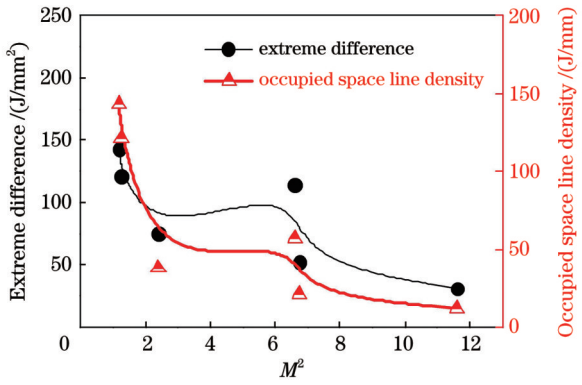

图 6 M^2对能量密度极值差和占空线密度的影响。(a)极值差;(b)占空线密度

Fig. 6 Influence of M^2 on extreme difference in energy density and occupied space line density. (a) Extreme difference; (b) occupied space line density

成能量在两侧累积,导致熔池向两侧分散,进而造成能量流动[23]。激光能量密度的极大值是激光能量密度分布的一种表征方式,激光能量密度的分布影响工件温度场的分布,即激光能量密度的极大值决定了温度场的平衡情况,进而影响焊接过程中能量的流动与吸收,所以将激光器能量密度极大值和能量密度极值差两者的乘积作为激光器能量密度的焊接效率影响因子。经过计算可以得到,M^2为 1.18 时激光器能量密度的焊接效率影响因子比M^2为 11.60 时的增加了 5.2 倍。同时,为了便于分析焊道两端极大值和中间极小值之间的面积差异,将能量分布图中极大值和中间极小值之间的面积定义为激光能量占空线密度,M^2为 1.18 时的激光能量占空线密度比M^2为 11.60 时的增加了 10.7 倍。

基于上述能量分布特征和能量密度的分析结果,激光器光束质量效应的提升机制如下。

激光器的光束质量不仅影响激光器的光斑大小,还影响摆动激光焊接过程中能量密度的极值差和能量分布的均匀性。从上文可知,M^2为 11.60 时激光器的光斑大小比M^2为 1.18 时的增加了 7.3 倍,与此同时,激光器的能量密度也出现较大变化。在采用圆形摆动模式后,在保持相同熔深的条件下,不同焊接速度下的激光能量分布也出现很大差异,尤其是焊道边缘的能量密度较大,中间区域的较小,两者的能量密度极值差越大,工件材料的能量吸收效率会越高,进而激光器的焊接效率越大。M^2为 1.18 时激光器能量密度的焊接效率影响因子比M^2为 11.6 时的增加了 5.2 倍,这与实验测得的焊接效率提升倍数基本接近,说明激光器能量密度的焊接效率因子和激光器的焊接效率是正相关的。另外,激光焊接过程中激光能量分布的均匀性直接影响激光的稳定性,进而影响激光器焊接的良率。在圆形摆动激光焊接能量分布 YOZ图中,光束的圆形摆动造成能量累积,激光能量密度分布呈现焊道左右两边高、中间低的现象[24],而且两端的能量密度极值峰越陡峭,中间区域的能量分布越均匀,即激光器M^2越小,激光能量密度占空面积越大,激光能量的整体分布越均匀,激光焊接过程也就越稳定,因此焊接良率越高,焊接CPK值也就越大。

4 结 论

基于激光焊接过程中的能量分布特征,系统分析了铝合金焊接中的光纤激光器光束质量效应,建立了光束质量与焊接稳定性和焊接效率的定量关系,得到以下结论。

1) 当激光器的光纤芯径为 50 μm 和 100 μm 时,在相同的焊接速度下,M^2越小,焊缝的熔深越大,而焊缝的熔宽变化越小;当光纤芯径为 20 μm 时,M^2对焊缝熔深和熔宽的影响较小。

2) 随着激光器M^2的减小,焊缝熔深为 2.7 mm 时对应的焊接速度呈增大趋势,焊接熔深CPK值也呈增大趋势;当M^2从 11.6 减小到 1.25 时,焊缝熔深为 2.7 mm 时对应的激光器的焊接速度增加了 5.5 倍,焊接熔深CPK值提升了 2.3 倍。

3) 基于激光能量分布特征的分析结果,激光器光束质量效应的提升机制为:采用圆形摆动模式后,在保持相同熔深的条件下,M^2越小,能量密度极大值越大,且焊道边缘与中间区域之间的能量密度极值差越大,工件材料的能量吸收效率会越高,则激光器的焊接效率越高。综合考虑激光器能量密度极大值和能量密度极值差的影响,提出将两者的乘积作为激光器能量密度的焊接效率影响因子。由理论计算可知,M^2为 1.18 时激光器能量密度的焊接效率影响因子比M^2为 11.60 时的增加了 5.2 倍,与实验结果基本一致。

参 考 文 献

[1] Zhu X D, Li W. The pricing strategy of dual recycling channels for power batteries of new energy vehicles under government subsidies [J]. Complexity, 2020, 2020: 1-16.

[2] Yu H J, Dai H L, Tian G D, et al. Big-data-based power battery recycling for new energy vehicles: information sharing platform and intelligent transportation optimization[J]. IEEE Access, 2020, 8: 99605-99623.

[3] Shen H Y, Hou F. Trade policy uncertainty and corporate innovation evidence from Chinese listed firms in new energy vehicle industry[J]. Energy Economics, 2021, 97: 105217.

[4] Yuan X L, Liu X, Zuo J. The development of new energy vehicles for a sustainable future: a review[J]. Renewable and Sustainable Energy Reviews, 2015, 42: 298-305.

[5] 王瑜, 舒乐时, 耿韶宁, 等. 汽车车身激光焊接技术的现状与发展趋势[J]. 中国激光, 2022, 49(12): 1202004.
Wang Y, Shu L S, Geng S N, et al. Present situation and development trend of laser welding technology for automobile body [J]. Chinese Journal of Lasers, 2022, 49(12): 1202004.

[6] 郭少锋, 代小光, 彭杨, 等. 14 μm 芯径 2 kW 光纤振荡器及紫铜焊接试验研究[J]. 激光与光电子学进展, 2022, 59(21): 2136002.
Guo S F, Dai X G, Peng Y, et al. Experimental study on 14 μm core diameter 2 kW fiber oscillator and copper welding[J]. Laser & Optoelectronics Progress, 2022, 59(21): 2136002.

[7] 张迪, 赵琳, 刘奥博, 等. 激光能量对激光焊接接头熔化形状、气

孔和微观组织的影响及其调控方法[J]. 中国激光, 2021, 48(15): 1502005.
Zhang D, Zhao L, Liu A B, et al. Understanding and controlling the influence of laser energy on penetration, porosity, and microstructure during laser welding[J]. Chinese Journal of Lasers, 2021, 48(15): 1502005.
[8] 张高磊, 孔华, 邹江林, 等. 高功率光纤激光深熔焊接飞溅特性以及离焦量对飞溅的影响[J]. 中国激光, 2021, 48(22): 2202008.
Zhang G L, Kong H, Zou J L, et al. Spatter characteristics of high-power fibre laser deep penetration welding and effect of defocus on spatter[J]. Chinese Journal of Lasers, 2021, 48(22): 2202008.
[9] Zhou X H, Zhao H Y, Liu F Y, et al. Effects of beam oscillation modes on microstructure and mechanical properties of laser welded 2060 Al-Li alloy joints[J]. Optics & Laser Technology, 2021, 144: 107389.
[10] 耿立博. 汽车动力电池盖板激光焊接工艺研究[D]. 哈尔滨: 哈尔滨工业大学, 2017: 9-23.
Geng L B. Study on laser welding technology of automobile power battery cover plate[D]. Harbin: Harbin Institute of Technology, 2017: 9-23.
[11] 王天鸽, 唐新华, 韩潇潇, 等. 5083铝合金真空激光焊缝成形的影响因素[J]. 中国激光, 2018, 45(11): 1102001.
Wang T G, Tang X H, Han X X, et al. Factors influencing weld formation for laser welding of 5083 aluminum alloy in vacuum[J]. Chinese Journal of Lasers, 2018, 45(11): 1102001.
[12] 邹吉鹏, 李连胜, 宫建锋, 等. 铝合金厚板激光扫描填丝焊接气孔抑制[J]. 焊接学报, 2019, 40(10): 43-47, 66, 163.
Zou J P, Li L S, Gong J F, et al. Aluminum alloy thick plate laser scanning wire filling welding porosity suppression[J]. Transactions of the China Welding Institution, 2019, 40(10): 43-47, 66, 163.
[13] Huang L J, Hua X M, Wu D S, et al. Experimental investigation and numerical study on the elimination of porosity in aluminum alloy laser welding and laser-GMA welding[J]. Journal of Materials Engineering and Performance, 2019, 28(3): 1618-1627.
[14] Shaikh U F, Das A, Barai A, et al. Electro-thermo-mechanical behaviours of laser joints for electric vehicle battery interconnects [C]//2019 Electric Vehicles International Conference (EV), October 3-4, 2019, Bucharest, Romania. New York: IEEE Press, 2019.
[15] Dimatteo V, Ascari A, Liverani E, et al. Experimental investigation on the effect of spot diameter on continuous-wave laser welding of copper and aluminum thin sheets for battery manufacturing[J]. Optics & Laser Technology, 2022, 145: 107495.
[16] Wang L, Gao M, Zhang C, et al. Effect of beam oscillating pattern on weld characterization of laser welding of AA6061-T6 aluminum alloy[J]. Materials & Design, 2016, 108: 707-717.
[17] Zubiri F, del Mar Petite M, Ochoa J, et al. Welding optimization of dissimilar copper-aluminum thin sheets with high brightness lasers[M]//Boellinghaus T, Lippold J C, Cross C E. Cracking phenomena in welds IV. Cham: Springer, 2016: 219-228.
[18] 张羽昊, 陈辉, 杨策, 等. 激光功率对铝合金激光-MIG复合焊熔滴过渡行为及飞溅的影响[J]. 激光与光电子学进展, 2022, 59(17): 1714005.
Zhang Y H, Chen H, Yang C, et al. Effect of laser power on droplet transfer behavior and splash in aluminum alloy laser-MIG hybrid welding[J]. Laser & Optoelectronics Progress, 2022, 59(17): 1714005.
[19] 林文虎, 吴岳, 李芳, 等. 振镜扫描激光焊接QP1180高强钢的组织和性能研究[J]. 中国激光, 2022, 49(22): 2202015.
Lin W H, Wu Y, Li F, et al. Study on microstructure and properties of QP1180 high strength steel welded by vibrating mirror scanning laser[J]. Chinese Journal of Lasers, 2022, 49(22): 2202015.
[20] Schultz V, Seefeld T, Vollertsen F. Gap bridging ability in laser beam welding of thin aluminum sheets[J]. Physics Procedia, 2014, 56: 545-553.
[21] Hornik P, Šebestová H, Novotný J, et al. Laser beam oscillation strategy for weld geometry variation[J]. Journal of Manufacturing Processes, 2022, 84: 216-222.
[22] Shi W T, Li J H, Liu Y D, et al. Experimental study on mechanism of influence of laser energy density on surface quality of Ti-6Al-4V alloy in selective laser melting[J]. Journal of Central South University, 2022, 29(10): 3447-3462.
[23] Shi L, Li X, Jiang L H G, et al. Numerical study of keyhole-induced porosity suppression mechanism in laser welding with beam oscillation[J]. Science and Technology of Welding and Joining, 2021, 26(5): 349-355.
[24] Wang L, Gao M, Zeng X Y. Experiment and prediction of weld morphology for laser oscillating welding of AA6061 aluminium alloy[J]. Science and Technology of Welding and Joining, 2019, 24(4): 334-341.

Effects of Beam Quality on Laser Welding Efficiency and Yield of Aluminum Alloy

Zhang Shuai[1,2], Liu Tongzheng[1], Xu Zhihong[1], Dai Xiaoguang[1], Zhu Zhaohui[1], Gao Ming[2*], Guo Shaofeng[1]

[1]*Hunan Dake Laser Company Limited, Xiangyin* 414615, *Hunan, China*;

[2]*Wuhan National Laboratory for Optoelectronics* (*WNLO*), *Huazhong University of Science and Technology, Wuhan* 430074, *Hubei, China*

Abstract

Objective To achieve carbon neutrality, lithium batteries, as a new generation of green energy products, are poised to enter the terawatt-hour (TW·h, equivalent to 1000 GW·h) era. Currently, mainstream manufacturers of state-of-the-art energy batteries have reached a production capacity of 200 pieces per minute (PPM), and there are plans to increase the production capacity of cylindrical batteries to 300 PPM. Consequently, extremely high-speed production lines present substantial challenges to the welding process.

Therefore, the development of highly efficient and reliable battery-welding technologies and processes has become an urgent concern for the automobile manufacturing industry. Laser welding, with its small laser spot, high energy density, efficient welding, precise energy control, automation capabilities, and safety features, has been widely used in the field of new energy battery welding, including vehicle manufacturing. Recent research has primarily focused on enhancing the welding quality of aluminum alloys by optimizing laser welding process parameters and beam shaping. However, as the demand for higher welding efficiency in power battery welding increases, the scope for ensuring both welding quality and speed becomes constrained, making it increasingly challenging to identify suitable process parameters. Considering that lasers, as a new type of welding light source, exhibit characteristics distinct from those of the arc light sources generated by arc welding machines, research has primarily focused on laser power. The impact of laser light source characteristics on welding quality and efficiency, particularly the influence of laser beam quality, has received limited attention. To meet the demands of high-speed production lines for new energy power batteries, the effect of the beam quality from fiber lasers in aluminum alloy laser welding is systematically analyzed in this study based on the energy distribution characteristics within the laser welding process. The quantitative relationship between beam quality and welding stability, as well as welding efficiency, is also explored.

Methods An industrial-grade 3-kW continuous fiber laser is used in the experiment. The laser employs a circular swing path for welding with a swing amplitude of 0.6 mm and spacing of 0.25 mm. The upper-layer material consists of a 1.5-mm-thick 3003 aluminum alloy plate, while the lower-layer material is a 3-mm-thick 3003 aluminum alloy plate.

Results and Discussions With a decrease in the laser beam quality factor (M^2), the welding speed increases, corresponding to the same weld penetration (2.7 mm), and the complex process capability index (CPK) value of weld penetration also increases. When the M^2 is reduced from 11.6 to 1.25, the welding speed increases by 5.5 times, and the CPK value of the weld penetration increases by 2.3 times, corresponding to the same weld penetration (2.7 mm) (Fig. 4). Analyzing the energy distribution of postlaser welding oscillations on the YOZ surface reveals that, as the M^2 improves, there is a consistent downward trend in the maximum value of the laser energy density. In addition, the area between the two maximum values decreases. For instance, the maximum energy density at M^2=1.18 is 1.4 times higher than that at M^2=11.6 (Fig. 5). To gauge the influence of the laser energy density on the welding efficiency, a factor derived from the product of the maximum laser energy density and the difference in the maximum value of the energy density is introduced. Calculations demonstrate that, at M^2=1.18, this influence factor for laser energy density welding efficiency is 5.2 times higher compared with that at M^2=11.6 (Fig. 6). To facilitate the assessment of the area disparities between the maximum peak and intermediate minimum at both ends of the weld, the region between these points on the energy distribution map is defined as the laser energy occupied space line density. Remarkably, when M^2 is 1.18, the laser energy occupied space line density is 10.7 times greater than that when M^2 is 11.6 (Fig. 6).

Conclusions The influence of the beam quality from fiber lasers on aluminum alloy welding is systematically analyzed by considering the energy distribution characteristics during the welding process. A quantitative relationship between beam quality and welding stability, as well as welding efficiency, is established. The improvement mechanism for the laser beam quality effect is as follows. When the M^2 decreases while retaining the same penetration depth, the maximum value of the energy density increases, and the energy density between the edge of the weld bead and the middle interval also increases. The higher the energy absorption efficiency of the workpiece material, the higher the welding efficiency of the laser. The product of the maximum value of the laser energy density and the difference in the maximum value of the energy density is used as a factor influencing the laser energy density welding efficiency. The theoretical calculations show that, when M^2 is 1.18, the influence factor of the laser energy density welding efficiency is 5.2 times higher than that when M^2 is 11.6, which is basically consistent with the experimental results.

Key words laser technique; laser welding; beam quality; energy distribution; aluminum alloy